

Wear and Degradation Modes in Selected Vehicle Tribosystems

G. Pantazopoulos^a, A. Tsolakis^b, P. Psyllaki^b, A. Vazdirvanidis^a

^aELKEME Hellenic Research Centre for Metals S.A., 252 Pireaus Str., 17778 Athens, Greece,

^bLaboratory of Tribology, Department of Mechanical Engineering, Technological Education Institute of Piraeus (TEI of Piraeus), 250 Thivon Avenue, 122 44, Egaleo, Greece.

Keywords:

Pressure plate
Cast-iron
Shear stress
Brake disk
Stainless steel
Radial crack
Fatigue

A B S T R A C T

The wear and degradation mechanisms of two principle vehicle tribosystems are presented to elucidate the main causes of their premature failure. The first case study concerns the malfunction of an automotive cast iron pressure plate operated in an automobile clutch system. The second is related to the unexpected failure of a stainless steel brake disk of a high performance motorcycle. Both components are designed to function under sliding friction conditions that lead to the severe wear of consumable non-metallic parts of the tribosystems: the clutch disk and the brake pad, respectively. However, in both cases it was the unexpected failure of the conjugate metallic parts that resulted in terminal system damage. The experimental approach to identify the root cause of failure involved both microstructure characterization, as well as observations of the metallic contact surfaces by means of optical and scanning electron microscopy, in conjunction with microhardness and surface topography measurements. For the case of the stainless steel brake disk in particular, Finite Element Analysis was employed to simulate the operating tribosystem, identify the site(s) prone for crack initiation and validate the failure mechanisms hypotheses.

© 2015 Published by Faculty of Engineering

1. INTRODUCTION AND BACKGROUND

The proper operation of all type of vehicles requires the incorporation of several assemblies, the main function of which is based on the conjugate motion of parts in contact. Such tribosystems, like gearboxes or clutch and brake systems, are key elements for critical vehicle operations concerning power transmission, gear shifting, braking, etc.

The continuously increasing safety levels together with weight minimization for fuel economy purposes constitute principal strategies in modern vehicle design and manufacturing. Thus, in the competitive industrial and market environment a growing demand exists for high performance, yet cost-efficient, construction materials, operating under severe service conditions (high friction, increased loads and temperatures). The quality

and reliability of the vehicle's structural components affect significantly maintenance costs and driving safety. Even though vehicle manufacturers provide life-time expectancies of all separate critical assemblies, sudden or premature failures, which could have serious implications on the vehicles' integrity and passengers' safety, cannot be completely eliminated, primarily due to the random mechanical loading conditions that depend on individual's driving attitude and/or highly alternating traffic situations. This fact renders the failure analysis of such distinct cases an indispensable tool for designers and manufacturers. Root-cause analysis implemented in robust manufacturing and quality systems aims to identify the causal factors of failure and determine corrective and preventive actions to minimize or even eliminate the risk for future incidents.

Due to the crucial significance of the vehicles good-function on the safety of human beings, the relevant international interest has been shifted to the integration of experimental findings on catastrophic failure of such parts / components / sub-assemblies in the relevant Quality Assurance planning of the entire engineering system. This integration is implemented via Failure Mode and Effect Analysis (FMEA) accompanied by Failure Tree Analysis (FTA) methodologies that are carried out at the early stages of the system design. In this integration, all the potential failure-causes of the system's constitutive parts are hierarchically evaluated in a measurable way as possible incidents. In the case of vehicles' drum brakes, the application of the above mentioned approach permits ranging of elements' failure modes according to their severity and constitutes a powerful Quality Assurance Tool for the choice of the proper correction / elimination / prevention actions [1].

In the present work, the investigation of wear and degradation mechanisms of two main vehicle tribosystems is presented, elucidating the crucial aspects of the damage evolved. The first case concerns the study of the mechanisms that caused severe wear of an automotive metallic clutch pressure plate in contact with a consumable glass-fiber-reinforced-polymer-matrix composite disk (Fig. 1). This tribosystem enables gear shifting in the drive train. A sudden and premature malfunction of the clutch

assembly triggered a failure investigation for determining the root-cause. Microscopic observations on the contact surface of the grey cast iron pressure plate revealed the activation of various wear modes, such as severe sliding wear, groove formation and oxidation, whereas observations on cross-sections indicated also sub-surface damage. Furthermore, the most plausible hypothesis on cause of failure was constructed together with the suggested preventive actions [2]. The second case study is related to the unexpected failure of a high performance motorcycle's stainless steel brake disk, operating in contact to a ceramic-particle-metal-matrix composite brake pad (Fig. 2a). Radial cracking initiated at the ventilation holes in the outer area of the hardened brake disk (Fig. 2c). Microscopic observations combined with Finite Element Analysis (FEA) revealed the synergy between a fatigue mechanism as a result of thermomechanical stresses field developed because of random braking, and the expected wear of the conjugated parts.

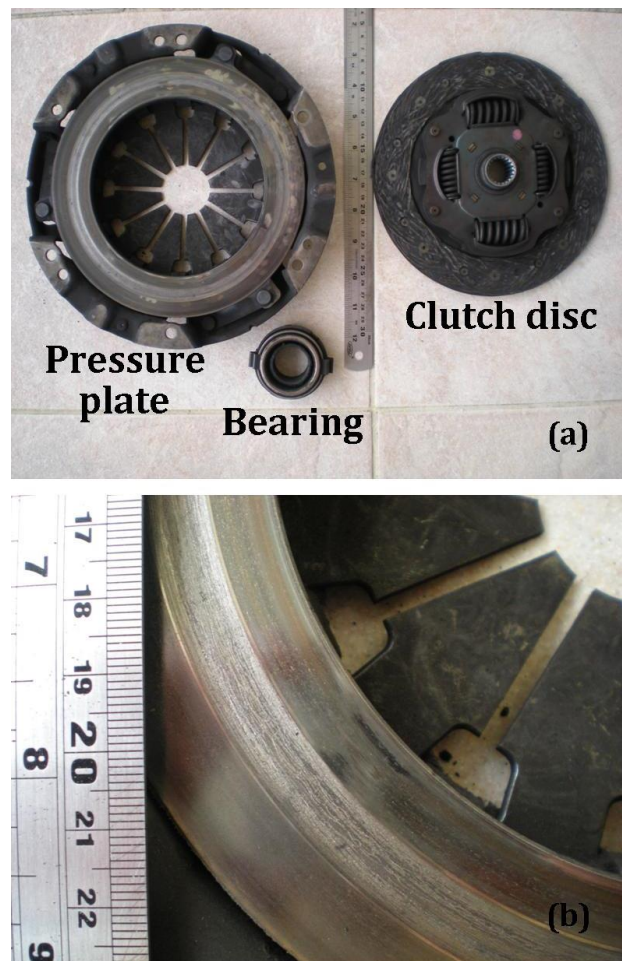


Fig. 1. Macro-graph of the failed (a) Clutch assembly, (b) Metallic pressure plate (detail).

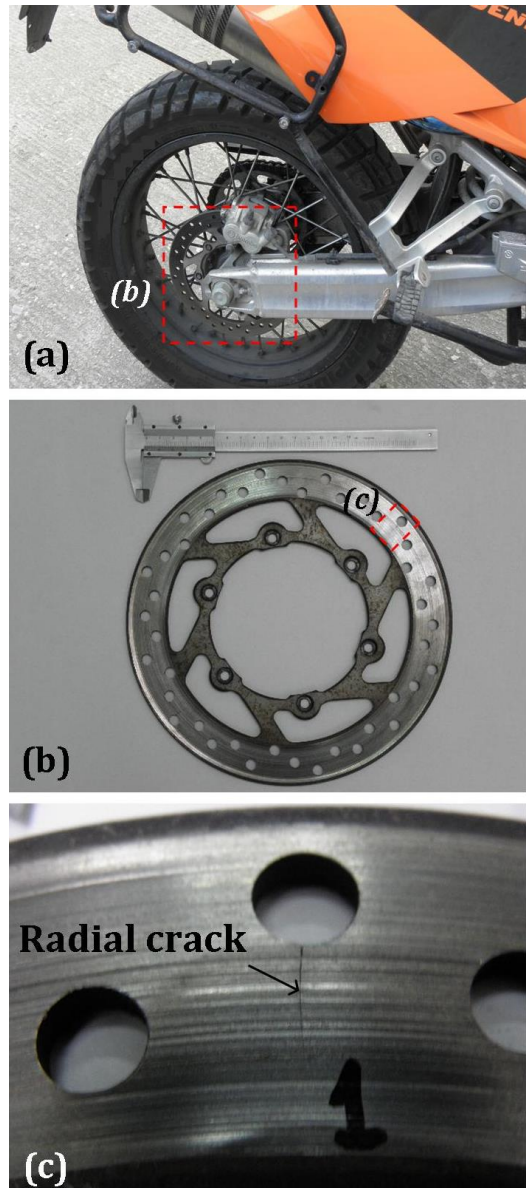


Fig. 2. (a) Motorcycle braking assembly, (b) Metallic brake disk failed, (c) Detail of (b).

2. EXPERIMENTAL TECHNIQUES

Macroscopic observations of the failed parts were conducted using a Leica MS 5 and a Nikon SMZ 1500 stereomicroscope. Roughness measurements of the worn surface were carried out using a mechanical Taylor-Hobson stylus profilometer and a Wyko NT1100 3-D optical profiler. In order to reveal the main failure mechanisms, microscopic observations were carried out using an FEI XL40 SFESEM Scanning Electron Microscope (SEM) equipped with secondary and backscattered electron detectors and an Electron Dispersive X-ray Spectrometer (EDS) for elemental micro-analysis of selected

areas. Chemical composition of the examined metallic components was determined via Optical Emission Spectroscopy (OES).

Metallographic examination was conducted using a Nikon Epiphot 300 inverted metallographic microscope. Prior to that, cross-sections of the specimens were prepared using hot-mounting, wet grinding up to 1200 grit SiC paper and polishing with diamond and silica suspensions. Chemical etching was performed by immersion of the cast-iron and stainless steel specimens in 2% Nital and aqua regia reagents, respectively, followed by cleaning with ethanol and drying in hot-air stream. Vickers microhardness measurements on characteristic areas of the specimens were carried out using an Instron-Wolpert microhardness tester, applying a load of 1 kg.

3. FINDINGS AND DISCUSSION

3.1 Pressure plate/ clutch disk tribosystem

The premature failure of the clutch assembly concerned its unexpected lost of function after ~40.000 km of service that necessitated its immediate replacement. A general remark in the case of the retrieved metallic pressure plate is that its entire surface has been affected during service. Surface areas, which had not been in contact to the clutch disk, exhibited discoloration, indicative of local oxidation (Fig. 1b). Even if these areas are not actually parts of the tribocouple, are affected by the heat dissipation from their neighbouring heavily loaded contact area. On the contact area, a ~10 mm-wide wear track was formed (Figs. 1b, 3a and 4), exhibiting a surface relief consisting of a sequence of deep valleys and crests (Fig. 3b). The stereo-microscopic observations of the wear track (Figs. 3a, 3c), as well as the optical-microscopic ones (Fig. 3d), indicated severe dragging and deep grooving along the sliding direction, as the main wear modes accompanied by micropolishing and microcutting. Such mechanisms are common in tool and bearing materials, as reported in the relevant literature [3-6]. The oblong deep grooves observed are consistent with the roughness measurements at various locations along the wear track (Fig. 3b), that allowed the determination of their mean dimensions as ~3 mm in width and ~0,2 mm in depth.

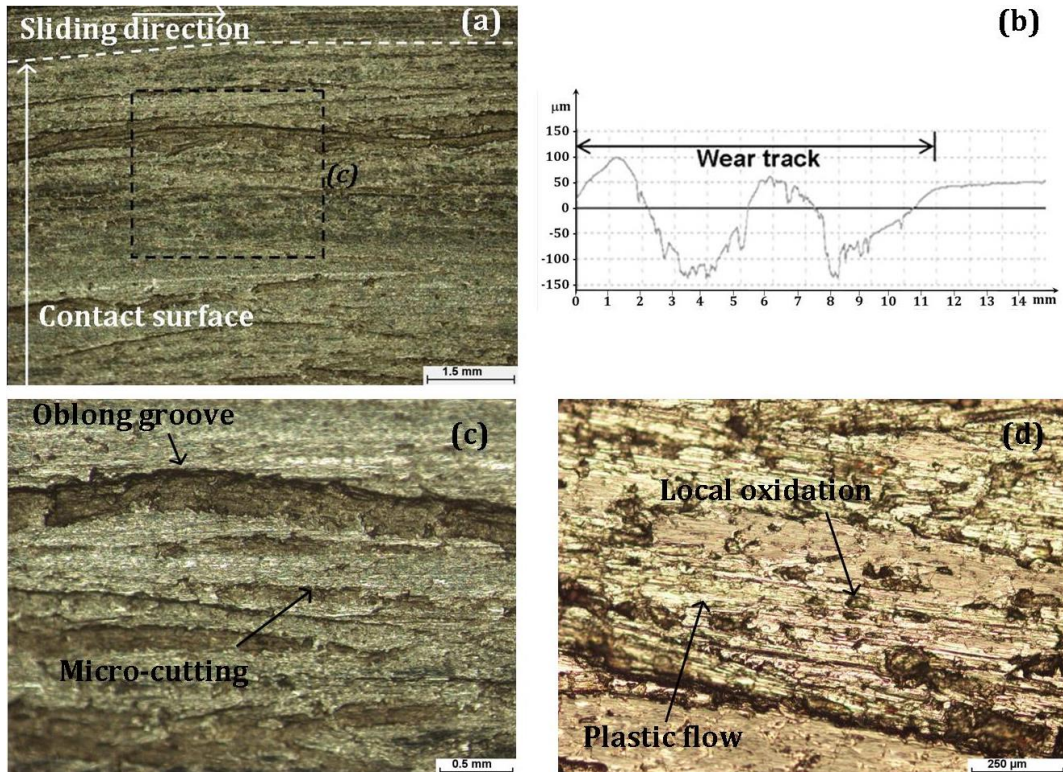


Fig. 3. Characteristics of the worn surface of the pressure plate: (a) Top view stereo-micrograph, (b) Surface profile across the entire wear track, (c) Stereo- and (d) Optical-micrographs showing details of the wear mechanisms.

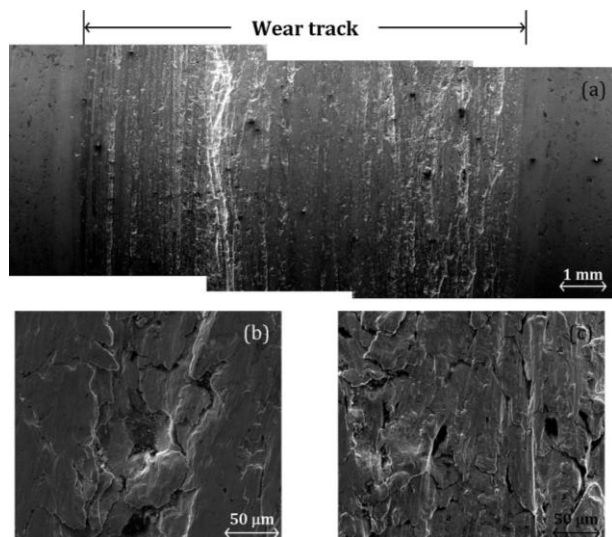


Fig. 4. SEM micrographs of (a) the wear track formed on the contact area and (b) and (c) magnifications of characteristic areas within it.

Further SEM observations within the wear track showed a random presence of voids, with average dimensions of 30 μm, as well as severe plastic flow of the metal along the sliding direction (Fig. 4). The presence of voids suggests the occurrence of prior ductile tearing of the surface under high stress state followed by crack opening and growth, leading to smearing under the operation conditions of the tribosystem.

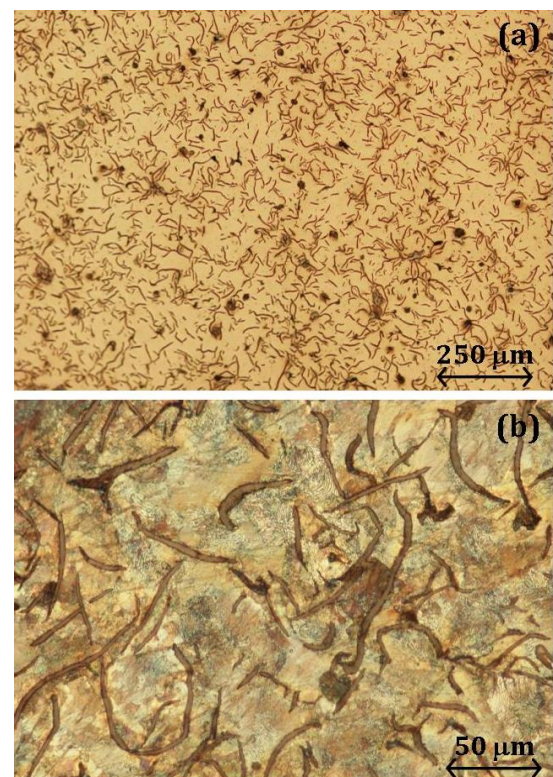


Fig. 5. (a) Optical micrographs of the pressure plate initial microstructure and (b) magnification of (a).

Metallographic observation of cross-sections transverse to the wear track indicated that the pressure plate was fabricated from gray cast

iron, with graphite flakes dispersed in a ferrite-pearlite matrix (Fig. 5). The microhardness values corresponding to this microstructure varied from 220 to 240 HV1, with the higher ones measured underneath the worn surface, indicating possible associated work hardening due to plastic deformation imposed on a thin surface layer of the pressure plate.

SEM observations combined with EDS analysis on cross-sections revealed also in-depth oxidation of the metallic surface (Fig. 6), due to heat evolution during sliding friction. Thermo-mechanical numerical simulations via finite element analysis of similar clutch plates operating under dry sliding conditions indicated temperature raises in the order of 150-250 °C, after 10 repeated engagements [7,8]. In the particular case presented in this study, such a temperature increase can render the metallic plate more prone to oxidation, whilst the expansion of the oxidation layer could be attributed to even higher temperature increase associated to more severe operational conditions, probably applied accidentally. This surface oxide layer due to its brittleness enables flaking and spalling mechanisms, which in turn amplify material removal from these specific areas, creating secondary grooves of approximately the same dimensions. The morphology and the dimensions of the oxidized areas and the grooves advocates for these being consecutive instants of a complementary wear micro-mechanism of the friction surface that acted in synergy to the overall surface deterioration: under loading which leads to overheating, the metallic surface is locally oxidized with the oxidation advancing preferentially within the ferrite-pearlite matrix [2]. During sliding, the shear stresses developed in the brittle oxide result in cracking of the oxide layer followed by its removal from the metallic plate, leaving surface pits and grooves.

Microscopic observation of cross-sections transverse to the contact area revealed also that the pressure plate degradation is not limited only to surface phenomena, but is in-depth extended. In Fig. 7, crack initiation at graphite flakes edges [9] well below the worn surface and its propagation within the ferrite-pearlite matrix in a direction parallel to the contact surface is clearly observed, not only in the higher-magnification SEM micrograph but is also

evident in the optical one. The depth, at which these cracks are observed, was in all cases of the order of 20-30 µm, corresponding almost precisely to the depth at which maximum shear stress was established for the particular operating conditions and system configuration, according to Hertz contact stress theory [5].

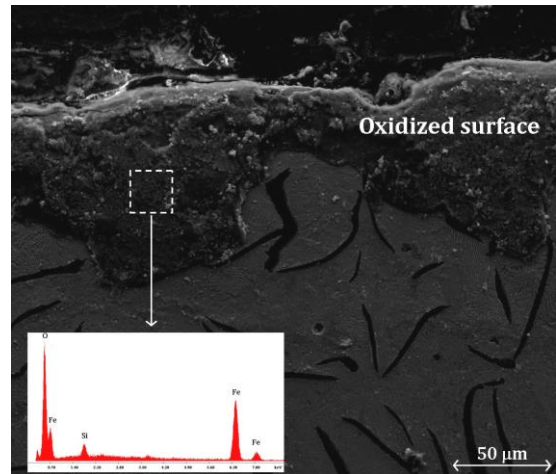


Fig. 6. Near contact surface SEM micrograph of cross-section and corresponding EDS analysis on the area marked, indicating local in-depth oxidation.

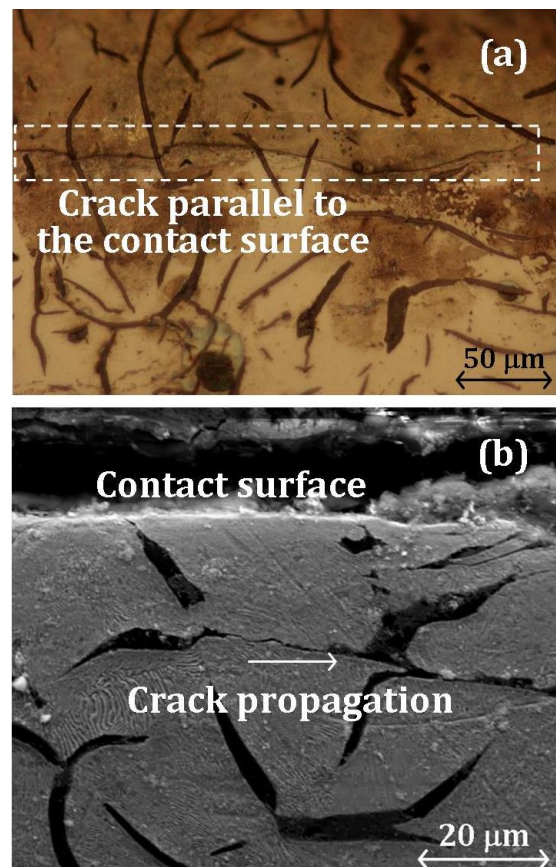


Fig. 7. (a) Optical and (b) SEM micrographs of cross-sections indicating crack propagation parallel to the contact surface within the metallic matrix.

3.2 Brake disk/ brake pad tribosystem

Control of wear in clutch and brake vehicle tribosystems is of paramount importance for safe and reliable driving performance [10]. The progressive consumption of the consumable component, in this case the brake pad, requires its replacement within regular intervals during periodic maintenance. However, the brake disk is also subjected to wear, even though in significantly lower wear rate, and according to the manufacturers specifications, the used brake disk should be replaced when a specific reduction of its thickness is reached.

The present case concerns the premature failure of a brake disk operating in a high performance motorcycle. The component under study is a single body, comprised however of two distinct parts, like all similar components: the first (bridge) attaches firmly the component on the wheel and transmits the braking torque to it; the second (flange) is the main part of the component that participates in the tribosystem being in contact with the consumable part during the braking process. To address the issue of thermal loads developed during their operation, the flanges carry ventilation holes of various shapes and arrangements [11]. As already shown in Fig. 2b, the ventilation holes of this particular disk are arranged in a 3-2-2 pattern, repeated 6 times in total. Despite the fact that during periodic maintenance, the disk thickness reduction was within acceptable levels ($\sim 0,6$ mm < 1,0 mm according to the manufacturer's specification), radial cracks emanating only from the outmost ventilation holes were identified (Fig. 8). Similar failure findings have also been reported and studied recently [12].

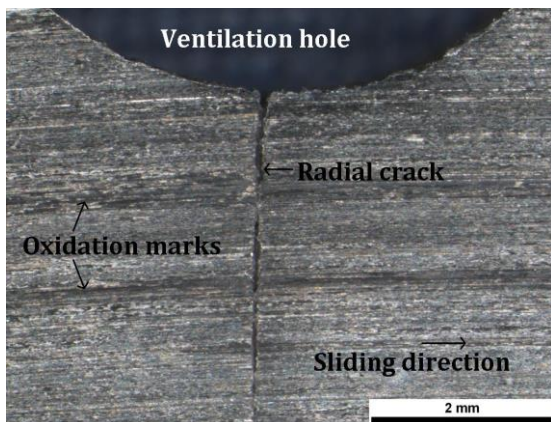


Fig. 8. Stereo-micrograph of failed area, depicting a radial crack emanating from a ventilation hole.

The chemical composition of the disk material indicated that the disk was manufactured of stainless steel matching approximately the AISI 410 grade (Table 1).

Table 1. Chemical composition of the brake disk material (% wt.)

C	Ni	Cr	Mn	Si	Mo	V	Fe
0,06	0,16	12,7	1,52	0,30	0,05	0,02	Bal.

Optical and SEM evaluation of cross-sections of the brake disk showed a fine-grained (~ 10 μm) microstructure on both bridge and flange areas. More specifically the flange area (Fig. 9a), which constitutes the brake area in contact to the brake pad consisted of a hardened and tempered martensitic microstructure of a microhardness of 415 HV_{0,5} almost 100 HV_{0,5} higher than that of the bridge area (Fig. 9b).

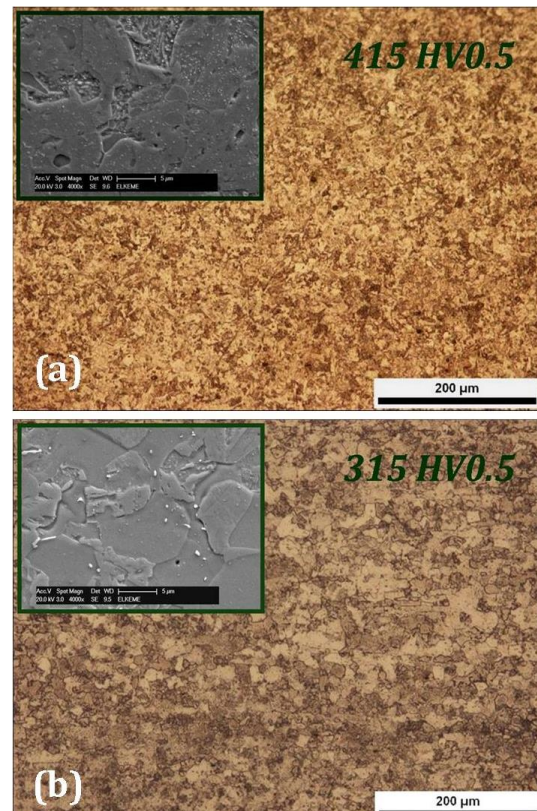


Fig. 9. Microstructure evolution of the stainless steel brake disk: (a) hardened and tempered structure of the flange area, (b) initial structure of the bridge area.

On the contact surface of the flange, clear traces of ploughing can be recognised corresponding to abrasive wear mechanisms due to the sliding contact of the ceramic particles reinforcement of the composite brake pad onto the stainless steel disk (Figs. 8, 10a). Isolated regions of severe

oxidation of the stainless steel were identified (Figs. 10a, 10b) indicative of local temperature raise above 600 °C during braking. 3-D optical profilometry measurements along the direction perpendicular to the wear track (Fig. 11a) determined the roughness characteristic parameters as follows: Ra=4.27 μm, Rq=4.93 μm, Rz=18.46 μm and Rt=18.83 μm. The almost linear shape of the respective Abbott-Firestone curve (Fig. 11b) demonstrated the constant wear rate during sliding, free from abnormal events.

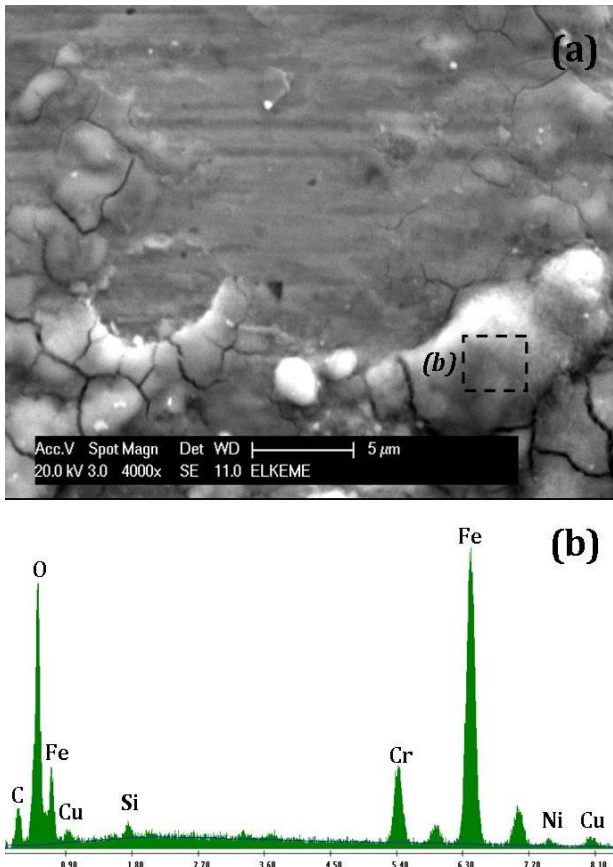


Fig. 10. (a) SEM micrograph of the flange contact surface indicating abrasive wear mechanism and isolated oxidation regions, (b) EDS analysis of the area marked in (a).

A specimen including the radial crack, as well as a significant non-affected area around it, was sectioned from the flange body, in order to observe the features of the created crack's fracture surface via SEM. In this respect, the radial non-affected area from the crack tip to the edge of the specimen was manually separated into two pieces by overloading. Fractographic evaluation of the conjugate surfaces indicated fatigue as the mechanism responsible for the crack initiation and propagation.

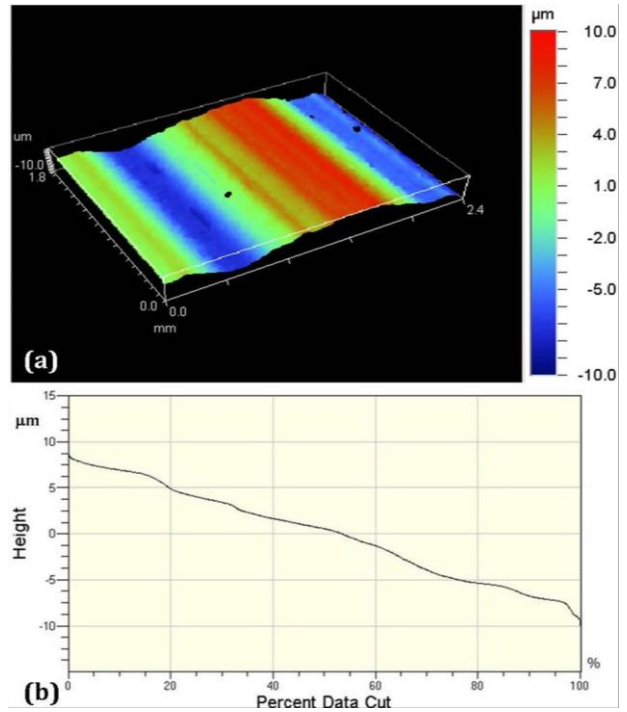
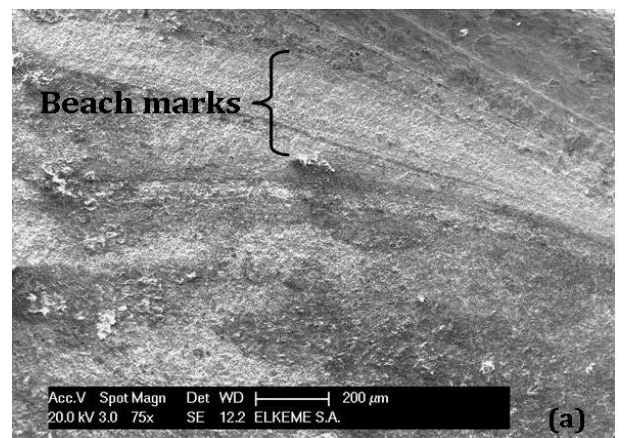


Fig. 11. (a) 3-D topography of the flange contact surface, (b) Respective Abbott-Firestone curve.

Fig. 12a presents fracture area adjacent to the ventilation hole. The presence of crack-arrestment marks, commonly known as beach marks, having occurred from intermittent loading is clear evidence of fatigue crack propagation via a flat and smooth front. Fig. 12b shows the fracture characteristics of the area adjacent to the crack tip. The striation-like pattern observed is typical signature of fatigue related to micro-plasticity processes at the crack tip (sharpening/blunting), and also depicts the local crack advancement per load cycle. Finally, Fig. 12c presents the area at the boundary between the crack propagation and post-crack-created overloaded area. The overloaded area consists of ductile shear (non-equiaxed) dimples coming from final ductile shear rupture.



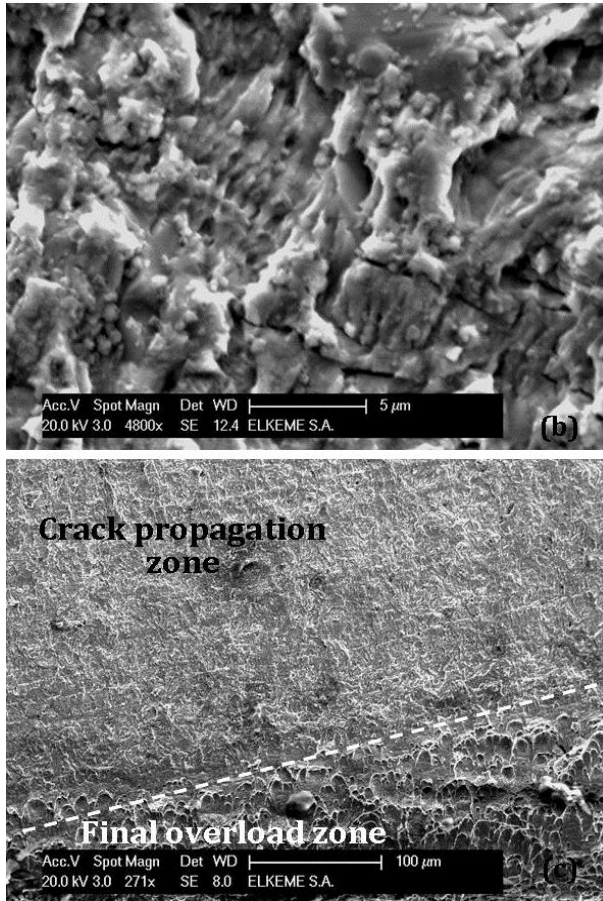


Fig. 12. Characteristic features on selected areas of the fracture surface: (a) Close to the ventilation hole, (b) Close to the crack tip, (c) At the interface between fatigue crack propagation and final overload area.

In order to address issues of crack initiation location only at the outermost ventilation hole, Finite Element Analysis was employed. In this perspective, preliminary simulations were performed for the "extreme" case of emergency braking conditions. In this case, the thermal effects can be considered negligible, so that only the mechanical (and not the entire "real" thermo-mechanical) effects can be taken into account. The whole brake disk was simulated by a global mesh of tetrahedral curved elements, more concentrated around the ventilation holes (Fig. 13a). For the calculations, a clockwise disk rotation was imposed, inducing a counter-clockwise friction force radial distribution. This friction force distribution was calculated based on "uniform pressure" theory [13]. The disk was assumed to be free of any prior mechanical and thermal loading. In the particular case of emergency braking conditions, under 35 bar pressure and an average friction coefficient of 0.53, as provided by the disk manufacturer, both von Mises and first principle stresses were calculated (Figs. 13b, 13c).

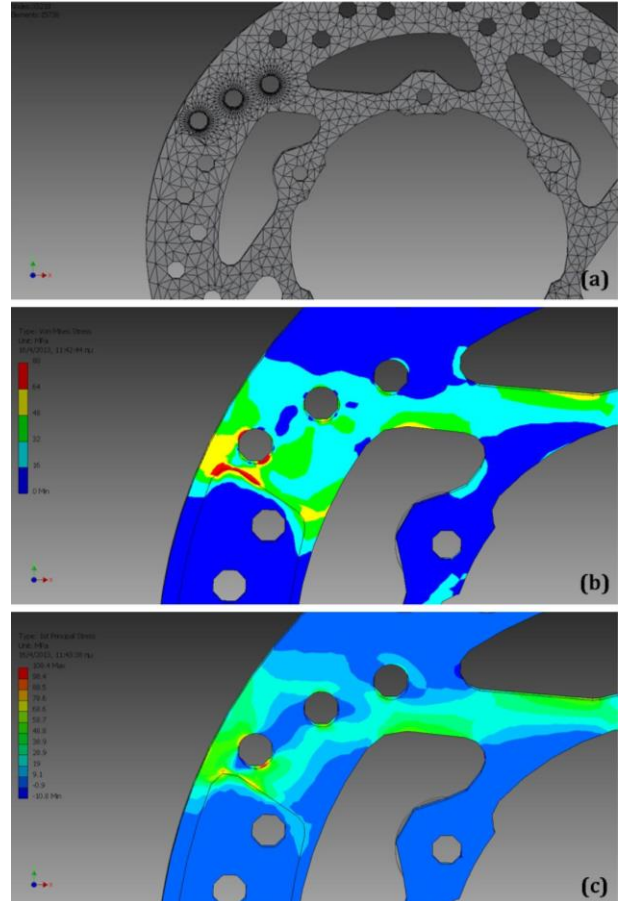


Fig. 13. Numerical simulation using Finite Element Analysis: (a) Global mesh of tetrahedral elements used, (b) Von Mises and (c) first principal, stress distribution contours.

It can be clearly seen that, indeed, the mechanical stresses present their maximum values at the outermost ventilation hole, where crack initiation and propagation was experimentally observed. More precisely, the maximum equivalent Von Mises and first principal stress found to be 80 and 108,4 MPa, respectively.

4. CONCLUSIONS AND RECOMMENDATIONS

The wear and degradation mechanisms of two principle vehicle tribosystems are presented to elucidate the main causes of their premature, unexpected failure of the conjugate metallic parts resulting in terminal system damage.

In the case of a cast iron pressure plate/clutch disk tribosystem, the metallic pressure plate has suffered from severe wear damage that progressed to catastrophic failure of the whole assembly. A thorough experimental evaluation

revealed the evolution of subsurface cracks propagating parallel to the worn surface during sliding and severe local oxidation of the metallic surface. The graphite flakes' morphology facilitates crack initiation and propagation within the pearlite matrix. Preventive maintenance, scheduled periodically or just after an overload incident is suggested as the main measure to manage safety risks.

In the case of a stainless steel brake disk/brake pad tribosystem, both experimental studies, as well as FEA results corroborated that fatigue cracks could emanate from the outermost ventilation holes of the brake disk, which are the most highly loaded areas prone to fracture. The main disk surface wear mechanisms include micropolishing, ploughing and oxidative wear as a result of thermomechanical loading during sliding. Further research could be recommended towards possible disk design revision and/or alternative material selection exhibiting higher thermomechanical fatigue strength, satisfying severe loading conditions during braking and optimizing the life expectancy of the vehicle tribosystem.

REFERENCES

- [1] D. Ćatić, J. Glišović, J. Miković and S. Veličković, 'Analysis of failure causes and the criticality degree of elements of motor vehicle's drum brakes', *Tribology in Industry*, vol. 36, no. 3, pp. 316-325, 2014.
- [2] P. Psyllaki, G. Pantazopoulos and P. Karaiskos, 'Failure mechanisms of an automobile clutch assembly cast iron pressure plate', *Journal of Failure Analysis and Prevention*, vol. 12, no. 1, pp. 16-23, 2012.
- [3] P. Psyllaki, G. Kefalonikas, G. Pantazopoulos, S. Antoniou and J. Sideris, 'Microstructure and tribological behaviour of liquid nitrocarburized tool steels', *Surface and Coatings Technology*, vol. 162, no. 1, pp. 67-78, 2003.
- [4] G. Pantazopoulos, T. Papazoglou, P. Psyllaki, G. Sfantis, S. Antoniou, K. Papadimitriou and J. Sideris, 'Sliding wear behaviour of a liquid nitrocarburised precipitation-hardening (PH) stainless steel', *Surface and Coatings Technology*, vol. 187, no. 1, pp. 77-85, 2004.
- [5] G. Pantazopoulos, P. Psyllaki, D. Kanakis, S. Antoniou, K. Papadimitriou and J. Sideris, 'Tribological properties of a liquid nitrocarburised special purpose cold-work tool steel', *Surface and Coatings Technology*, vol. 200, no. 20-21, pp. 5889-5895, 2006.
- [6] I.M. Hutchings, *Tribology: Friction and Wear of Engineering Materials*, Edward Arnold, London, 1992.
- [7] O.I. Abdullah and J. Schlattmann, 'Finite element analysis of temperature field in automotive dry friction clutch', *Tribology in Industry*, vol. 34, no. 4, pp. 206-216, 2012.
- [8] O.I. Abdullah, J. Schlattmann and A.M. Al-Shabibi, 'Thermo-mechanical analysis of the dry clutches under different boundary conditions', *Tribology in Industry*, vol. 36, no. 2, pp. 172-180, 2014.
- [9] E.E. Vernon, M.E. Stevenson, J.L. McDougall and L. McCall, 'Failure analysis of gray iron pump housings', *Journal of Failure Analysis and Prevention*, vol. 4, no. 6, pp. 15-18, 2004.
- [10] Y. Yildiz and M. Duzgun, 'Stress analysis of ventilated brake discs using the finite element method', *International Journal of Automotive Technology*, vol. 11, no. 1, pp. 133-138, 2010.
- [11] R. Thornton, T. Slatter, A.H. Jones and R. Lewis, 'The effects of cryogenic processing on the wear resistance of grey cast iron brake discs', *Wear*, vol. 271, no. 9-10, pp. 2386-2395, 2011.
- [12] M. Boniardi, F.D. Errico, C. Tagliabue, G. Gotti and G. Perricone, 'Failure analysis of a motorcycle brake disc', *Engineering Failure Analysis*, Vol. 13, No 6, pp. 933-945, 2006.
- [13] R.I. Norton, *Machine Design: An Integrated Approach*, 3rd Ed. Prentice-Hall Inc. New Jersey, 2005.